

# Geochemistry of Carboniferous low metamorphic grade sedimentary and tholeiitic igneous rocks in the western Acatlán complex, southern Mexico: deposition along the active western margin of Pangea

Carlos Ortega-Obregón<sup>1</sup>, J. Duncan Keppie<sup>1,\*</sup>, J. Brendan Murphy<sup>2</sup>

<sup>1</sup>Departamento de Geología Regional, Instituto de Geología, Universidad Nacional Autónoma de México, 04510 México D.F., Mexico.

<sup>2</sup>Department of Earth Sciences, St. Francis Xavier University, Antigonish, Nova Scotia, B2G 2W5a, Canada.

\*duncan@servidor.unam.mx

## ABSTRACT

*Low grade metasedimentary rocks in the western Acatlán complex (Olinalá area) of southern Mexico occur in two units termed here the Progreso and Zumpango units of Lower and middle Carboniferous ages, respectively. The Zumpango Unit is dominated by phyllite and quartzites, but the Progreso Unit is more highly deformed and is dominated by quartzite that is locally interbedded with pillow basalt, and intruded by a suite of mafic dikes. Geochemical and Sm-Nd isotopic data indicate that the basalts and the mafic dikes are tholeiitic, have N-MORB affinities and are moderately fractionated. Deposition of the Progreso Unit was coeval with Carboniferous extrusion of high metamorphic grade rocks of the Acatlán complex above of an active subduction zone, and deposition of Mississippian rocks in the adjacent Oaxaquia terrane. The tholeiitic affinity of mafic rocks, suggests extension on this active margin. The Mid-Continent (USA) affinities of the fauna in the latter rocks suggest that Pangea had already amalgamated and that these events took place on the western margin of Pangea.*

*Key words: geochemistry, active margin, Carboniferous, Pangea, Acatlán complex, Mexico.*

## RESUMEN

*Las rocas metasedimentarias de bajo grado en el complejo Acatlán occidental (área de Olinalá) del Sur de México, ocurren en dos unidades diferentes de cuarcitas y filitas denominadas aquí como Progreso y Zumpango de edad Carbonífero Inferior y medio, respectivamente. La Unidad Zumpango está caracterizada por filitas y cuarcitas, mientras que la Unidad Progreso, está formada principalmente por cuarcitas, localmente interestratificadas con basaltos almohadillados e intrusionadas por diques máficos, toleíticos con afinidades N-MORB y fraccionamiento moderado. El depósito de la unidad Progreso fue contemporáneo con la extrusión de las rocas metamórficas de alto grado del complejo Acatlán en una zona de subducción activa y con el depósito de rocas misisípicas en el margen del terreno Oaxaqueño adyacente. La afinidad toleítica de las rocas máficas sugiere extensión en esta margen activa. La afinidad meso-continental (EE.UU.) de la fauna en estas últimas sugiere que Pangea estaba ya amalgamada y que estos eventos tuvieron lugar en la margen occidental de Pangea.*

*Palabras clave: geoquímica, margen activo, Carbonífero, Pangea, Acatlán complex, México.*

## INTRODUCTION

The Acatlán complex, synonymous with the Mixteca terrane, underlies much of southern Mexico and its evolution provides important constraints for Late Paleozoic continental reconstructions along the western edge of Pangea (*e.g.*, Ortega-Gutiérrez *et al.*, 1999; Keppie and Ramos, 1999; Talavera-Mendoza *et al.*, 2005; Nance *et al.*, 2006, 2007; Vega-Granillo *et al.*, 2007; Keppie *et al.*, 2008a). Determination of the depositional setting of low-grade psammitic-pelitic and mafic rocks (originally assigned to the Cosoltepec Formation; Ortega-Gutiérrez *et al.*, 1999), which underlie *ca.* 60% of the Acatlán complex of southern Mexico is critical to the understanding of this evolution. Recent dating of detrital zircons in several samples from rocks assigned to this formation has shown it to be composite with both Ordovician and Devonian-Carboniferous units being present (Talavera-Mendoza *et al.*, 2005; Keppie *et al.*, 2006, 2008a; Ortega-Obregón *et al.*, 2009).

Although a rift-passive margin setting has been determined for the Ordovician units (Keppie *et al.*, 2006, 2008b; Ortega-Obregón *et al.*, 2009; Morales-Gómez *et al.*, 2009; Dostal and Keppie, 2009), the depositional setting of these rocks is still unclear and various models have been proposed. Talavera-Mendoza *et al.* (2005) have suggested that the Devonian-Carboniferous rocks were deposited along the passive margin of Gondwana (Amazonia-Oaxaquia). However, Keppie *et al.* (2008a) and Morales-Gómez *et al.* (2009) infer deposition in an active margin along the western side of Pangea. In an attempt to provide additional constraints, we present geochemical data for Carboniferous rocks in the western part of the Acatlán complex associated with clastic detritus derived mainly from the adjacent Oaxacan complex, Maya block and high grade metamorphic units of Acatlán complex (Ortega-Obregón *et al.*, 2009). Penetrative deformation synchronous with deposition suggests that these Carboniferous rocks were deposited along an active margin (Keppie *et al.*, 2008a, 2008b; Ortega-Obregón *et al.*, 2009). Given that the Rheic Ocean had all but closed by the beginning of the Carboniferous (Matte, 2001; Winchester *et al.*, 2002; Keppie *et al.*, 2008b), the active margin is inferred to have been located along the western margin of Pangea.

## GEOLOGICAL SETTING

The Acatlán complex is tectonically juxtaposed on its eastern, southern and western sides against the *ca.* 1 Ga Oaxacan and Mesozoic Xolapa complexes, and Cretaceous carbonates, respectively (Figure 1a). To the north, the complex is unconformably overlain by uppermost Devonian-Lower Permian rocks of the Patlanoya Group (Vachard *et al.*, 2000; Vachard and Flores-de Dios, 2002) and by Cenozoic rocks of the Trans-Mexican Volcanic Belt. As the geology (Keppie *et al.*, 2008a and references therein)

and detailed mapping supported by geochronology (Ortega-Obregón *et al.*, 2009) of the Olinalá area in the western part of the Acatlán complex has been recently published, we present only a summary of the western Acatlán complex geological record here.

1. Ediacaran to Lower-Middle Ordovician deposition of the Zacango Unit clastic rocks.
2. Ordovician intrusion into the Zacango Unit of *ca.* 465 Ma bimodal granitoids and amphibolites.
3. Lower-Middle Mississippian deposition of clastic rocks associated with mafic lavas and minor intrusions (Progreso Unit) that partially overlaps with latest Devonian-Middle Mississippian metamorphism, deformation and uplift/cooling through *ca.* 400 °C.
4. Upper Mississippian (-Lower Permian) deposition of clastic rocks and felsic ashes (Zumpango Unit).
5. Lower Permian low-grade deformation.
6. Middle-Upper Permian deposition of the Olinalá Formation, which consists of clastic units at the base that grade upward into calcareous clastic rocks.

7. Intrusion of a *ca.* 61 Ma diorite (lower Paleocene).  
This paper focuses on the Carboniferous Progreso and Zumpango units, previously mapped as part of the Cosoltepec Formation and Tecamate Formation (Ortega-Gutiérrez *et al.*, 1999, Ramírez-Espinoza, 2001, respectively). The Carboniferous Progreso Unit occurs in the Southern and Naranjo fault blocks (Figure 2). Deposition of this unit is bracketed by  $403 \pm 7$  Ma mean of three zircons and by a  $335 \pm 2$  Ma  $^{40}\text{Ar}/^{39}\text{Ar}$  age on metamorphic muscovite (Ortega-Obregón *et al.*, 2009). The Progreso Unit consists of pelitic and psammitic rocks interbedded with pillow lavas (Naranjo block) and intruded by mafic dikes (Southern block) that underwent greenschist facies metamorphism and polyphase deformation during the Carboniferous and Permian (Ortega-Obregón *et al.*, 2009). Despite the different age populations of zircons from these blocks (Naranjo and Progreso; Ortega-Obregón, *et al.*, 2009), the similar lithology, style of deformation and grade of metamorphism suggest contemporaneous deposition and tectonic evolution. In thin section, the psammitic-pelitic rocks exhibit a spaced foliation defined by microlithons of stretched quartz and fine grained white mica. The pillow basalts have hyalopilitic textures with very fine grained plagioclase laths, accessory opaque minerals, and chlorite microphenocrysts inferred to represent pseudomorphs after pyroxene, set in a greenish, extensively altered glassy matrix. The mineralogy indicates lower greenschist facies metamorphism.

The Progreso Unit is very similar in lithology, structure, and metamorphic grade to the Coatlico Unit, which crops out just to the southeast of Olinalá and consists of low-grade psammites, pelites and pillow basalts (Grodzicki *et al.*, 2008). The age of the the Coatlico Unit post-dates its youngest population of detrital zircons, dated at  $357 \pm 35$  Ma (Grodzicki *et al.*, 2008). The close lithological similarity between the Progreso and Coatlico units suggests that they are correlatives, implying that their deposition probably

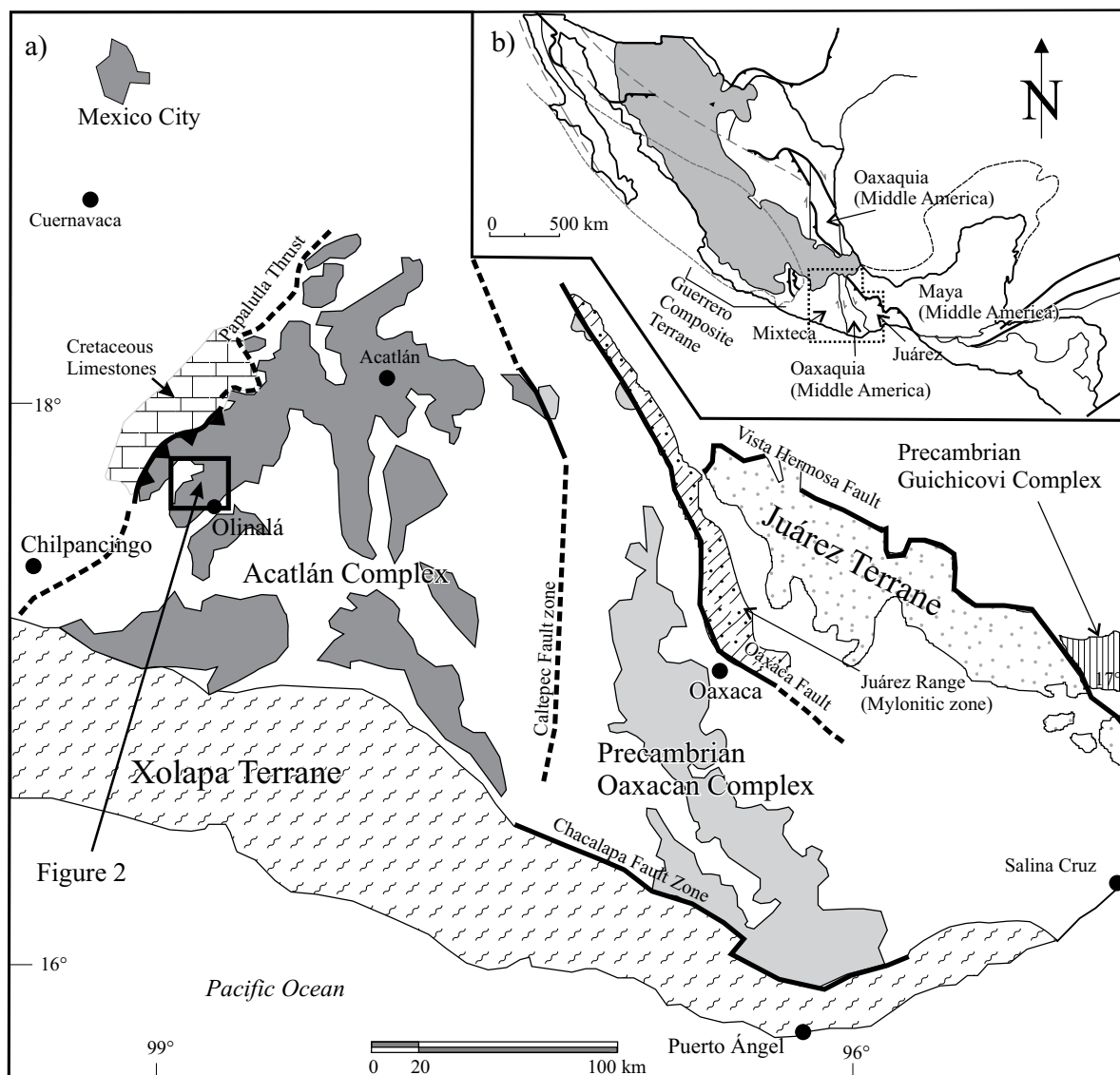


Figure 1. Terrane map of southern Mexico showing the locations of the Acatlán, Oaxacan and Xolapa complexes and the studied area at Olinalá, Guerrero (modified from Keppie *et al.*, 2008a).

post-dates the Devonian.

The Zumpango Unit occurs in two fault blocks and consists of sub-greenschist facies clastic rocks associated with felsic ash and minor mafic volcanic rocks (Figure 2). A volcanic epiclastic rock (felsic ash) within the Zumpango Unit yielded a single concordant zircon with an age of  $327 \pm 2$  Ma (upper Mississippian; Ortega-Obregón *et al.*, 2009). A maximum age for the clastic rocks deposited prior to this ash is partly constrained by the youngest detrital zircon in a psammite ( $348 \pm 3$  Ma) or the *ca.* 350–385 Ma of four crystals and the  $338 \pm 2$  Ma plateau age yielded by muscovite inferred as detrital (Ortega-Obregón *et al.*, 2009). No mafic rocks were found interbedded or intruding these metasedimentary rocks. The Zumpango Unit was deformed prior to deposition of the unconformably overlying Middle-Upper Permian Olinalá Formation (Vachard *et al.*, 2000).

## ANALYTICAL METHODS

In order to determine the tectonic setting of the Progreso Unit, 15 samples of the pillow basalts from the Naranjo block and one sample of a mafic dike from the Southern block (Figure 2) were analyzed for major and trace elements including rare earth elements (REE) along with four samples of the psammites and pelites. In addition, ten samples of metavolcanic felsic ashes and quartzites from the Zumpango Unit were also analyzed. The data are shown in Table 1.

Major and selected trace elements (Rb, Sr, Ga, Co, Cu, Pb, Zn, V, Cr and Ni) were determined by X-ray fluorescence spectrometry at the Nova Scotia Regional Geochemical Centre at Saint Mary's University, Nova Scotia using a Philips PW2400 X-ray spectrometer. Analytical

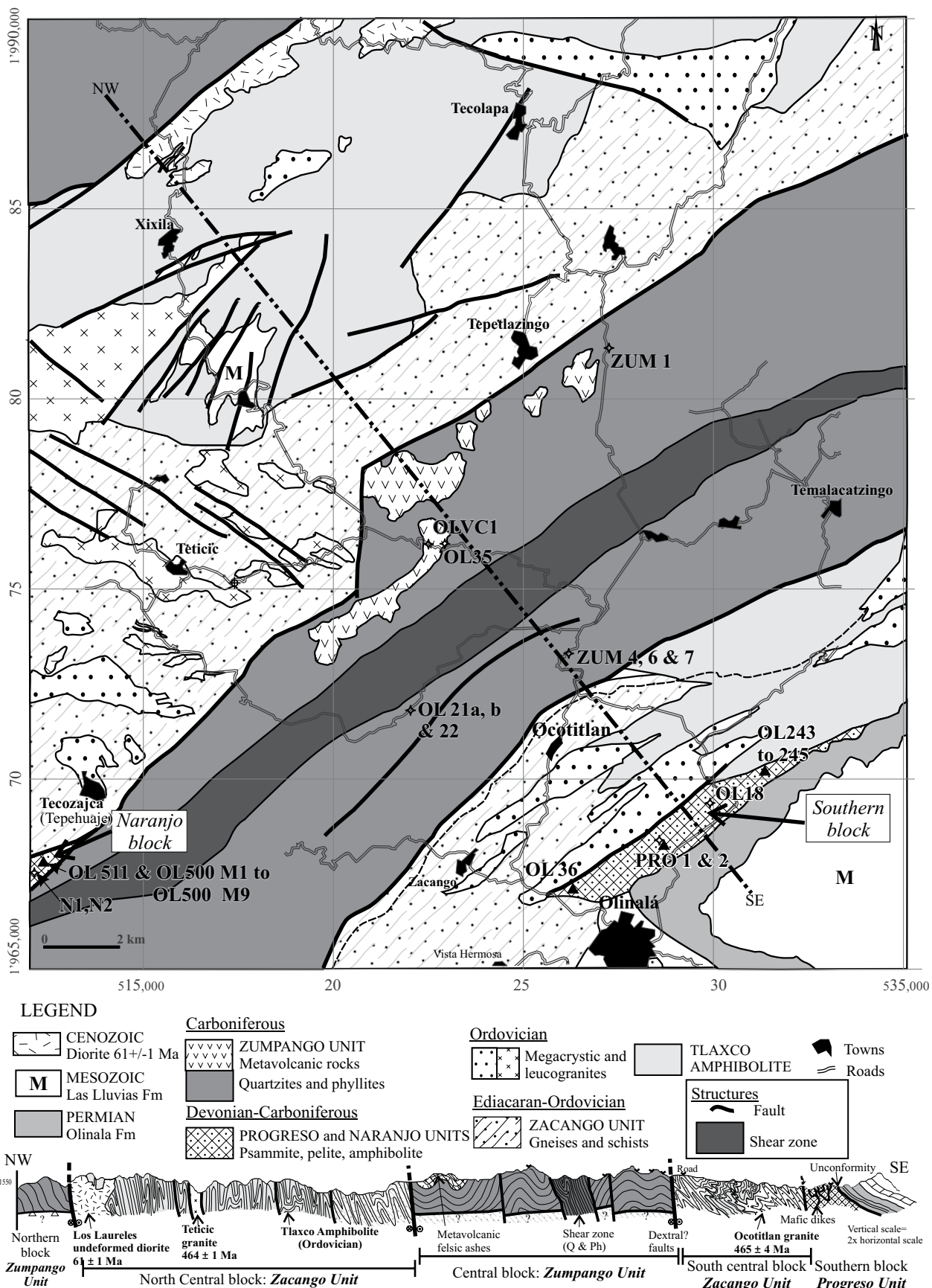


Figure 2. Simplified geological map and schematic section at the Olinalá region (modified from Ortega-Obregón *et al.*, 2009a).

procedures, precision and accuracy for the X-ray data are described by Dostal *et al.* (1994). Rare earth and other trace elements (Y, Zr, Nb, Cs, Ba, Hf, Th, U and Ta) and Sm-Nd isotopic analyses were determined at Memorial University, Newfoundland by Inductively Coupled Plasma-Mass Spectrometry (ICP-MS) and Isotope Dilution-Thermal Ionization Mass Spectrometry (ID-TIMS), respectively. Analytical methods are described in Jenner *et al.* (1990). Details of all geochemical analyses and analytical method are given in Table 1 (see footnote).

The Sm-Nd isotopic data from six samples of pillow basalts from the Naranjo block, as well as one sample of metasedimentary quartzite from the Progreso Unit and four samples of the Zumpango Unit are shown in Table 2. Details of the analytical procedures for the Sm-Nd isotopic analyses are described by Kerr *et al.* (1995). La Jolla Nd standard gave an average value of 0.511860.  $\epsilon$ Nd parameters were calculated relative to  $^{143}\text{Nd}/^{144}\text{Nd} = 0.512638$  and  $^{147}\text{Sm}/^{144}\text{Nd} = 0.196593$  for present day CHUR (Jacobsen and Wasserburg, 1980) and a decay constant  $\lambda^{147}\text{Sm} = 6.54 \times 10^{-12}/\text{year}$ . Nd Model ages [ $T_{\text{DM}}$ ] were calculated using the model of DePaolo (1981, 1988).  $\epsilon$ Nd values are calculated for  $t = 330$  Ma, which represents the probable extrusive age of mafic magmatic rocks.

## GEOCHEMICAL AND ISOTOPIC RESULTS

### Metasedimentary rocks

Results from the low grade metasedimentary rocks of the Progreso (including those from El Naranjo block; Figure 2) and Zumpango units were plotted together in order to assess their respective provenance. Both units show considerable variation in chemical composition, exemplified by the range in  $\text{SiO}_2$  from *ca.* 57.3 to 82.6 wt. % and *ca.* 70.2 to 92.1 wt.%, respectively (on a volatile free basis). Sample N2 from the Naranjo block, which has the lowest  $\text{SiO}_2$  value (*ca.* 57.3 wt%), was not plotted on geochemical diagrams due to its high loss of ignition (LOI) value (*ca.* 14.1 wt%; Table 1). MgO,  $\text{TiO}_2$  and Cr contents in Zumpango samples display negative correlations with  $\text{SiO}_2$  (Figure 3a, 3c and 3d). Although some samples from Zumpango Unit are detrital sedimentary rocks, this negative correlation could be inherited from a fractionated igneous felsic rock source. Positive correlations between some trace element ratios (*e.g.*, Ti/Y and Ti/V vs. Zr/Y and Zr/V; Figures 3e and 3f) suggest a contribution of minor phases (*e.g.*, zircon, magnetite and titanite) to the detritus. This suggests an important contribution from calc-alkaline granitoid rocks (*e.g.*, Murphy *et al.*, 2005).

Chondrite-normalized REE patterns for both metasedimentary units display moderate LREE enrichment relative to HREE with chondrite normalized  $(\text{La}/\text{Sm})_{\text{N}}$  varying from 4.8 and 6.3,  $(\text{La}/\text{Yb})_{\text{N}}$  varying from 11.2 to 14.1, and flat to slightly depleted HREE patterns (Figure 4a). These samples

also display a minor negative Eu anomaly ( $\text{Eu}_{\text{N}}/\text{Eu}^*$  ranges from 0.59 to 0.78). These features reflect the average of detrital contributions from the source area (*e.g.*, Murphy *et al.*, 1996). With the exception of low Sr, Nb and Ta, the REE and trace element abundances are similar to typical upper continental crust (Figure 4b). Negative anomalies in Nb and Ta may reflect source rock depletion (*i.e.*, derivation from arc-related rocks) whereas Sr negative anomalies may reflect weathering of feldspar.

Several geochemical features indicate that the clastic rocks were predominantly derived from felsic to intermediate source rocks: i) the enrichment in incompatible (*e.g.*, Th) relative to compatible trace elements (*e.g.*, Cr) is indicated by low Cr/Th (ranging from 0.3 to 5.3), values typical of a dominant felsic mixed with mafic source (Cullers, 1994); ii) the La/Th versus Hf diagram, where most rocks plot close to the field of the acid arc source (Figure 5; after Floyd and Leveridge, 1987); iii) the high  $\text{Al}_2\text{O}_3/\text{TiO}_2$  values of six of the ten Zumpango Unit samples ( $>20$ ) also suggest derivation from predominantly felsic sources (*e.g.*, Girty *et al.*, 1996); and; iv) the relatively low contents of  $\text{Fe}_2\text{O}_3$  and MgO in some samples (Table 1). The negative Nb and Ta anomalies evident in Figure 3b, suggest that these felsic rock sources were produced in a magmatic arc.

All metasedimentary samples have relatively homogeneous Sm-Nd isotopic characteristics, with  $\epsilon$ Nd ( $t = 330$  Ma) of -6 in Progreso quartzite and a range from -7.5 to -8.4 in the Zumpango Unit samples. Ratios of  $^{147}\text{Sm}/^{144}\text{Nd}$  of all samples range from 0.1156 to 0.1242. Depleted mantle model age ( $T_{\text{DM}}$ , DePaolo, 1981) of the Progreso Unit quartzite is 1.7 Ga and range from 1.66 to 1.82 Ga in the Zumpango Unit samples (Table 2).

### Progreso Unit mafic rocks

Despite the well preserved shapes of the Progreso pillow basalts, secondary processes (such as alteration and metamorphism) have affected the primary concentrations of many major and some trace elements. The effects of alteration are indicated by the high loss on ignition (LOI) in several samples (*e.g.*, OL36-1, OL36-2 and OL500-M1), and by the scatter of data points on diagrams containing alkali and alkali-earth elements, indicating that many of the primary characteristics of the basalts have been modified. We therefore describe the major element abundances only in very general terms, and focus on the abundances of selected trace elements, such as high field strength (HFSE) and rare earth (REE) elements, which are both considered to be "relatively" immobile during hydrous alteration (*e.g.*, Winchester and Floyd, 1977; Pearce, 1996).

The pillow basalts range in  $\text{SiO}_2$  content between 47.6 to 52.6 wt% (on a volatile free basis). Pillow basalts have a relatively homogeneous geochemical composition and on most diagrams generally plot in a cluster. Mg# (= molar  $\{\text{MgO}/[\text{MgO}+\text{Fe}_2\text{O}_3]\}$ ) ranges between 32.8 and 58.4

Table 1. Chemical analysis of low metamorphic grade mafic and metasedimentary rocks of Progreso and Zumpango units.

Sample	Metabasalts									
	OL-36(1)	OL-36(2)	OL-243	OL-244	OL-245	OL-500 M1	OL-501 M2	OL-502 M3	OL-503 M4	OL-504 M5
UTM N	1,966,917	1,966,917	1,970,191	1,970,168	1,970,206	1,968,234	1,968,232	1,968,229	1,968,230	1,968,226
UTM E	526,469	526,469	531,779	531,817	531,786	514,345	514,342	514,341	514,342	514,338
SiO <sub>2</sub> (wt%)	47.0	45.8	47.4	48.7	46.2	43.3	47.4	46.1	46.8	46.6
TiO <sub>2</sub>	1.67	1.27	1.31	1.04	1.36	1.45	1.02	1.49	1.45	1.33
Al <sub>2</sub> O <sub>3</sub>	22.7	18.3	15.9	14.6	15.7	15.3	14.4	15.3	15.4	14.7
Fe <sub>2</sub> O <sub>3</sub>	13.5	10.9	10.6	11.6	12.3	10.6	12.4	12.4	12.1	12.4
MnO	0.12	0.15	0.17	0.14	0.16	0.15	0.15	0.16	0.17	0.18
MgO	3.7	6.0	7.8	7.3	7.4	6.7	7.6	7.3	7.0	7.8
CaO	0.4	4.7	9.0	9.5	10.0	9.4	10.5	10.1	10.4	10.6
Na <sub>2</sub> O	4.2	5.7	4.0	3.6	3.5	3.0	3.1	3.2	3.2	3.1
K <sub>2</sub> O	2.80	0.14	0.33	0.14	0.17	0.21	0.09	0.09	0.09	0.09
P <sub>2</sub> O <sub>5</sub>	0.13	0.11	0.12	0.12	0.13	0.19	0.11	0.13	0.12	0.12
Mg#	32.8	49.7	56.9	52.7	51.7	52.9	52.2	51.4	50.9	52.8
L.O.I.	5.1	7.0	3.3	3.4	3.1	9.7	3.2	3.6	3.4	3.0
Total	106.3	100.1	96.7	96.6	96.9	90.3	96.8	96.4	96.6	97.1
V (ppm)	201	276	315	305	311	300	297	303	318	305
Cr	374	356	250	290	281	348	276	285	303	281
Co	81.0	67.0	59.4	56.2	48.9	40.3	47.6	48.1	48.4	40.4
Ni	104	112	105	104	100	157	105	101	106	98
Cu	13	39	129	124	131	78	123	132	138	128
Zn	104	86	86	85	87	96	89	91	87	84
Ga	22.0	18.0	15.4	12.8	16.2	19.0	16.6	15.0	17.6	15.7
Rb	74.0	8.0	11.2	6.2	4.8	21.2	5.5	4.3	4.6	4.2
Sr	53	250	367	87	255	185	228	133	89	68
Y	32	24	18	21	21	30	20	21	22	21
Zr	103	75	78	83	81	171	80	84	85	81
Nb	3.7	3.3	5.4	5.6	5.6	8.0	5.5	5.8	6.0	5.7
Cs	n.d.	n.d.	n.d.	2.8	n.d.	17.9	3.9	6.7	n.d.	3.8
Ba	629	50	104	54	78	97	36	40	30	28
La	2.6	1.9	4.1	4.4	4.6	13.7	4.4	4.8	4.6	4.7
Ce	6.3	6.0	11.2	11.8	11.8	31.5	12.2	12.1	12.2	11.8
Pr	1.04	1.31	1.75	1.85	1.78	4.33	1.68	1.88	1.91	1.70
Nd	5.9	8.4	8.9	8.9	8.8	19.3	9.5	9.8	9.4	9.6
Sm	2.4	3.5	2.7	2.9	2.7	5.0	2.8	2.9	3.2	3.2
Eu	0.82	1.17	1.16	1.09	1.10	1.58	1.05	1.17	1.07	1.07
Gd	4.3	4.3	3.8	3.7	3.5	5.7	3.4	3.8	4.0	3.7
Tb	0.82	0.78	0.60	0.67	0.60	0.94	0.60	0.62	0.68	0.59
Dy	5.8	5.2	4.0	4.5	4.2	5.8	3.9	4.3	4.3	4.2
Ho	1.26	1.09	0.76	0.85	0.86	1.25	0.86	0.91	0.85	0.91
Er	3.8	3.4	2.3	2.5	2.4	3.5	2.4	2.5	2.4	2.4
Tm	0.55	0.53	0.31	0.36	0.31	0.52	0.36	0.35	0.34	0.35
Yb	3.5	3.4	2.0	2.2	2.4	3.4	2.2	2.5	2.3	2.5
Lu	0.53	0.51	0.31	0.33	0.34	0.48	0.34	0.38	0.36	0.38
Hf	2.5	2.5	2.1	2.2	2.1	4.2	2.3	2.1	2.2	2.0
Ta	0.23	0.26	0.22	0.22	0.20	0.25	0.17	0.19	0.24	0.22
Pb	<3	<3	0.4	4.7	0.4	8.1	3.6	4.4	5.8	6.7
Th	0.35	0.33	0.38	0.31	0.32	2.64	0.32	0.40	0.35	0.39
U	4.0	3.0	0.0	4.3	3.4	0.0	5.7	3.1	1.1	0.3

Table 1 (continued). Chemical analysis of low metamorphic grade mafic and metasedimentary rocks of Progreso and Zumpango units.

Sample	Metabasalts					Progreso mafic dike	Progreso metasedimentary rocks			
	OL-505 M6	OL-506 M7	OL-507 M8	OL-508 M9	OL-509 M10	PRO-1	OL-511	N-1	N-2	PRO-2
UTM N	1,968,224	1,968,227	1,968,224	1,968,225	1,968,222	1,969,298	1,968,220	1,968,213	1,968,214	1,969,298
UTM E	5,143,439	514,339	514,339	514,338	514,342	527,342	5,143,439	514,334	514,334	527,342
SiO <sub>2</sub> (wt%)	46.5	47.3	48.0	46.8	46.6	50.8	81.1	74.7	49.1	73.4
TiO <sub>2</sub>	1.44	1.47	1.41	1.26	1.35	1.35	0.56	0.54	1.74	1.08
Al <sub>2</sub> O <sub>3</sub>	14.9	15.2	12.9	15.0	15.1	15.6	9.7	13.4	12.3	9.6
Fe <sub>2</sub> O <sub>3</sub>	12.5	12.4	11.8	12.3	12.5	9.7	2.0	3.6	10.2	5.5
MnO	0.18	0.17	0.14	0.17	0.17	0.18	0.09	0.04	0.15	0.09
MgO	7.5	7.4	9.1	8.0	7.5	7.6	0.5	0.9	5.0	1.2
CaO	10.6	9.3	11.7	10.0	10.1	7.0	0.5	0.2	4.3	1.8
Na <sub>2</sub> O	3.1	3.6	0.2	3.3	3.2	3.3	2.7	3.2	3.4	2.3
K <sub>2</sub> O	0.12	0.09	0.08	0.10	0.09	1.61	0.95	2.30	0.12	1.37
P <sub>2</sub> O <sub>5</sub>	0.12	0.12	0.12	0.12	0.12	0.15	0.06	0.10	0.17	0.09
Mg#	51.6	51.4	57.9	53.7	51.8	58.4	29.8	30.9	46.8	27.3
L.O.I.	3.0	3.0	4.6	3.0	3.2	3.5	2.0	1.9	14.5	2.9
Total	97.0	97.0	95.4	97.0	96.8	100.7	127.9	100.9	100.9	99.3
V (ppm)	315	313	293	289	305	278	51	60	327	83
Cr	290	278	271	267	281	315	41	38	70	29
Co	47.9	44.3	40.9	40.9	51.0	43.0	15.0	19.0	59.0	27.0
Ni	98	101	90	98	99	62	22	13	41	13
Cu	134	131	135	131	127	54	7	32	207	76
Zn	87	87	74	76	106	80	34	53	80	68
Ga	14.6	16.7	15.0	14.1	18.2	18.0	8.8	16.0	15.0	12.0
Rb	4.8	4.2	6.6	5.0	2.5	37.0	45.7	117.0	11.0	60.0
Sr	88	109	35	186	117	145	56	48	377	18
Y	21	21	18	21	21	26	14	45	29	23
Zr	80	82	86	83	82	118	179	209	95	311
Nb	5.4	5.7	6.0	5.9	5.7	9.0	7.9	11.0	1.0	19.3
Cs	2.8	3.0	4.8	2.0	0.0	n.d	0.0	n.d	n.d	n.d
Ba	38	44	21	25	34	390	224	510	248	344
La	4.5	4.6	4.7	4.7	4.5	35.0	18.6	45.0	72.0	37.0
Ce	11.4	12.0	11.3	12.2	11.6	n.d	42.8	n.d	n.d	52.0
Pr	1.77	1.82	1.64	1.89	1.76	n.d	4.53	n.d	n.d	6.35
Nd	9.0	9.6	8.6	9.6	9.8	36.0	16.8	39.0	62.0	38.0
Sm	2.8	3.0	2.7	2.8	2.8	n.d	3.3	n.d	n.d	5.7
Eu	1.10	1.13	1.02	1.13	1.05	n.d	0.65	n.d	n.d	1.44
Gd	3.9	3.8	3.4	3.9	3.8	n.d	2.9	n.d	n.d	5.3
Tb	0.61	0.64	0.56	0.62	0.63	n.d	0.42	n.d	n.d	0.83
Dy	4.2	4.1	3.9	4.3	4.2	n.d	2.9	n.d	n.d	4.9
Ho	0.82	0.82	0.80	0.87	0.86	n.d	0.57	n.d	n.d	1.00
Er	2.3	2.5	2.1	2.6	2.4	n.d	1.6	n.d	n.d	3.0
Tm	0.35	0.34	0.32	0.37	0.37	n.d	0.25	n.d	n.d	0.45
Yb	2.1	2.2	2.1	2.3	2.3	n.d	1.7	n.d	n.d	3.1
Lu	0.35	0.36	0.31	0.33	0.30	n.d	0.27	n.d	n.d	0.44
Hf	2.1	1.8	2.3	2.1	2.3	n.d	3.9	n.d	n.d	6.5
Ta	0.19	0.19	0.20	0.21	0.22	n.d	0.35	n.d	n.d	1.05
Pb	7.6	10.0	1.3	1.1	29.8	4.0	22.0	42.0	7.0	37.0
Th	0.35	0.33	0.41	0.35	0.35	4.00	6.7	27.0	7.0	7.3
U	2.6	2.3	1.2	1.3	2.9	2.0	2.4	5.0	4.0	4.0

Table 1 (continued). Chemical analysis of low metamorphic grade mafic and metasedimentary rocks of Progreso and Zumpango units.

Zumpango metasedimentary rocks										
Sample	OL-18B	OL-21A	OL-21B	OL-22	OL-35	OL-VC1	ZUM-1	ZUM-4	ZUM-6	ZUM-7
UTM N	1,969,621	1,971,721	1,971,721	1,971,756	1,976,289	1,976,359	1,981,792	1,973,434	1,973,520	1,973,545
UTM E	529,874	522,134	522,134	522,321	522,664	522,291	527,164	526,149	526,334	526,379
SiO <sub>2</sub> (wt%)	75.3	69.4	67.7	75.3	91.1	83.4	90.9	84.8	84.3	83.0
TiO <sub>2</sub>	0.71	0.76	0.82	0.53	0.26	0.38	0.23	0.37	0.33	0.46
Al <sub>2</sub> O <sub>3</sub>	12.7	15.3	16.3	12.1	4.3	10.2	5.7	7.8	10.2	9.1
Fe <sub>2</sub> O <sub>3</sub>	3.6	4.9	5.6	4.0	0.8	0.6	0.8	1.8	0.6	1.7
MnO	0.03	0.05	0.06	0.02	0.01	<0.001	0.00	0.01	<0.001	0.02
MgO	0.4	1.4	1.7	0.9	0.1	0.3	0.2	0.5	0.2	0.7
CaO	0.2	0.1	0.2	0.0	0.0	0.0	0.1	0.1	0.0	0.1
Na <sub>2</sub> O	2.8	1.6	1.5	1.4	0.8	1.1	1.0	1.7	<0.01	0.1
K <sub>2</sub> O	1.98	3.07	3.42	2.08	0.62	1.57	1.15	1.30	1.20	2.67
P <sub>2</sub> O <sub>5</sub>	0.11	0.09	0.15	0.07	0.02	0.02	0.05	0.08	0.04	0.03
Mg#	17.7	33.4	35.1	28.4	20.1	44.5	30.0	31.4	34.1	42.0
L.O.I.	2.7	3.4	3.6	3.5	1.1	2.5	0.7	1.2	2.9	2.7
Total	100.4	100.1	100.9	99.9	99.2	100.1	100.6	99.6	99.7	100.5
V (ppm)	50	92	100	66	14	32	23	28	22	48
Cr	20	55	63	35	21	13	21	15	14	27
Co	17.0	24.0	26.0	20.0	6.0	8.0	5.0	8.0	<5	8.0
Ni	<3	22	25	13	<3	<3	<3	<3	<3	<3
Cu	20	30	25	43	44	54	50	49	48	33
Zn	41	72	77	52	<5	17	6	19	<5	14
Ga	14.0	17.0	19.0	13.0	5.0	9.0	8.0	9.0	8.0	10.0
Rb	81.0	140.0	143.0	110.0	61.0	108.0	84.0	86.0	90.0	130.0
Sr	48	22	19	47	14	44	20	14	35	42
Y	36	32	30	27	47	64	9	43	56	47
Zr	418	182	182	200	406	245	195	313	369	393
Nb	28.0	18.8	20.2	14.6	11.0	15.0	5.6	7.0	18.0	19.0
Cs	n.d.									
Ba	365	577	672	377	28	213	102	113	152	426
La	41.0	56.0	62.0	51.0	18.0	33.0	18.0	33.0	37.0	42.0
Ce	n.d.	83.2	90.6	67.7	n.d.	n.d.	20.4	n.d.	n.d.	n.d.
Pr	n.d.	9.98	10.47	8.43	n.d.	n.d.	2.27	n.d.	n.d.	n.d.
Nd	33.0	52.0	59.0	45.0	<5	24.0	<5	17.0	19.0	27.0
Sm	n.d.	7.4	8.0	6.8	n.d.	n.d.	1.8	n.d.	n.d.	n.d.
Eu	n.d.	1.45	1.48	1.38	n.d.	n.d.	0.35	n.d.	n.d.	n.d.
Gd	n.d.	6.7	6.8	6.1	n.d.	n.d.	1.6	n.d.	n.d.	n.d.
Tb	n.d.	1.03	1.03	0.89	n.d.	n.d.	0.29	n.d.	n.d.	n.d.
Dy	n.d.	6.3	6.1	5.5	n.d.	n.d.	1.7	n.d.	n.d.	n.d.
Ho	n.d.	1.21	1.16	1.07	n.d.	n.d.	0.35	n.d.	n.d.	n.d.
Er	n.d.	3.5	3.3	2.9	n.d.	n.d.	1.1	n.d.	n.d.	n.d.
Tm	n.d.	0.50	0.49	0.42	n.d.	n.d.	0.17	n.d.	n.d.	n.d.
Yb	n.d.	3.2	3.2	2.6	n.d.	n.d.	1.1	n.d.	n.d.	n.d.
Lu	n.d.	0.46	0.47	0.39	n.d.	n.d.	0.20	n.d.	n.d.	n.d.
Hf	n.d.	4.0	3.9	3.8	n.d.	n.d.	3.2	n.d.	n.d.	n.d.
Ta	n.d.	1.39	1.47	0.91	n.d.	n.d.	0.28	n.d.	n.d.	n.d.
Pb	32.0	40.0	33.0	40.0	45.0	54.0	49.0	46.0	325.0	39.0
Th	26.0	13.7	15.1	10.3	36.0	37.0	3.9	35.0	39.0	32.0
U	5.0	4.0	4.0	5.0	7.0	7.0	7.0	6.0	7.0	6.0

n.d. = not determined. The analytical procedure for ICP-MS trace element analysis was as follows: (a) sintering of a 0.2 g sample aliquot with sodium peroxide, (b) dissolution of the sinter cake, separation and dissolution of REE hydroxide-bearing precipitate, (c) analysis by ICP-MS using the method of internal standardization to correct for matrix and drift effects. Full details of the procedure are given in Longerich et al. (1990). A pure quartz reagent blank and one or more certified geological reference standards [usually gabbro MRG-1 (CCRMP) and basalt BR-688 (NIST SRM 688)] were prepared and analyzed with samples. Reagent blank concentrations are generally insignificant and have not been subtracted from sample concentrations. Detection limits and reagent blanks are generally about 10% of chondrite values. Several inter-element interferences are present in ICP-MS analysis; the instrument was optimized such that for most rock types the interferences are at a sufficiently low level to be adequately corrected.

Table 2. Sm-Nd isotopic data for Carboniferous metasedimentary and mafic rocks of the Progreso and Zumpango units.

Sample	Nd (ppm)	Sm (ppm)	Sm/Nd	$^{147}\text{Sm}/^{144}\text{Nd}$	$^{143}\text{Nd}/^{144}\text{Nd}$	2s	$\epsilon\text{Nd}_{(0)}$	$\epsilon\text{Nd}_{(t=330)}$	$T_{\text{DM}}$ (Ma)
<i>Zumpango Unit</i>									
OL-21A	38.12	7.44	0.1950	0.1179	0.512035	5	-11.8	-8.4	1771
OL-21B	39.99	7.78	0.1944	0.1175	0.512047	5	-11.5	-8.2	1745
OL-22	32.80	6.74	0.2054	0.1242	0.512077	4	-10.9	-7.9	1824
ZUM-1	9.66	1.85	0.1911	0.1156	0.512079	5	-10.9	-7.5	1662
<i>Progreso Unit (Progreso block)</i>									
PRO-2	24.61	5.19	0.2107	0.1274	0.512179	5	-9.0	-6.0	1713
<i>Pillow basalts</i>									
OL-36(1)	5.39	2.18	0.4039	0.2442	0.513197	5	10.9	8.9	-
OL-36(2)	6.04	2.22	0.3683	0.2228	0.513179	5	10.6	9.5	-
OL-244	9.63	2.99	0.3101	0.1875	0.512956	4	6.2	6.6	-
OL-502M3	10.14	3.12	0.3075	0.1860	0.512958	4	6.3	6.8	-
OL-504M5	9.44	2.93	0.3099	0.1874	0.512937	4	5.8	6.2	-
OL-505M6	9.63	2.97	0.3077	0.1860	0.512939	7	5.9	6.4	-

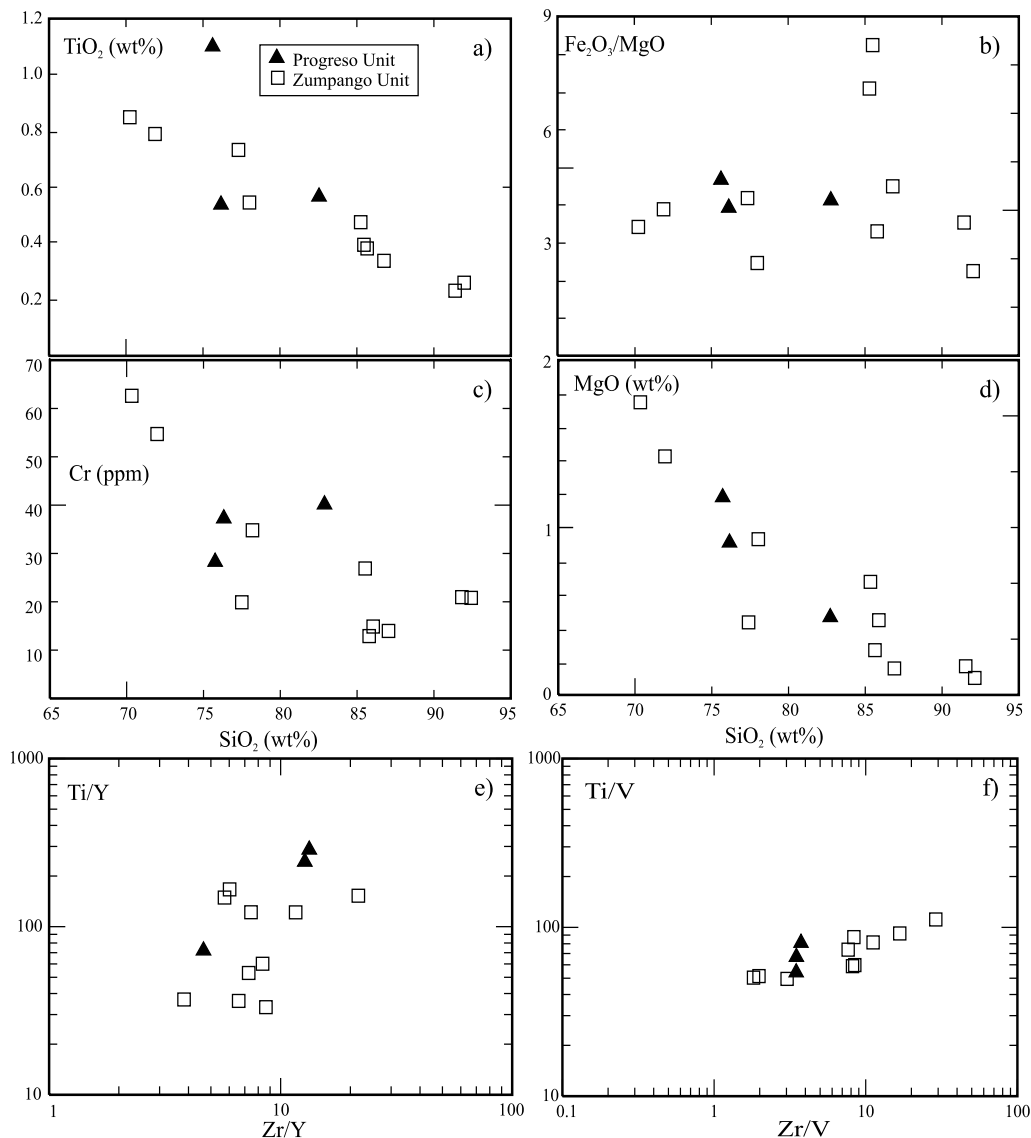


Figure 3. Major and trace element composition plots of Progreso and Zumpango metasedimentary rocks.

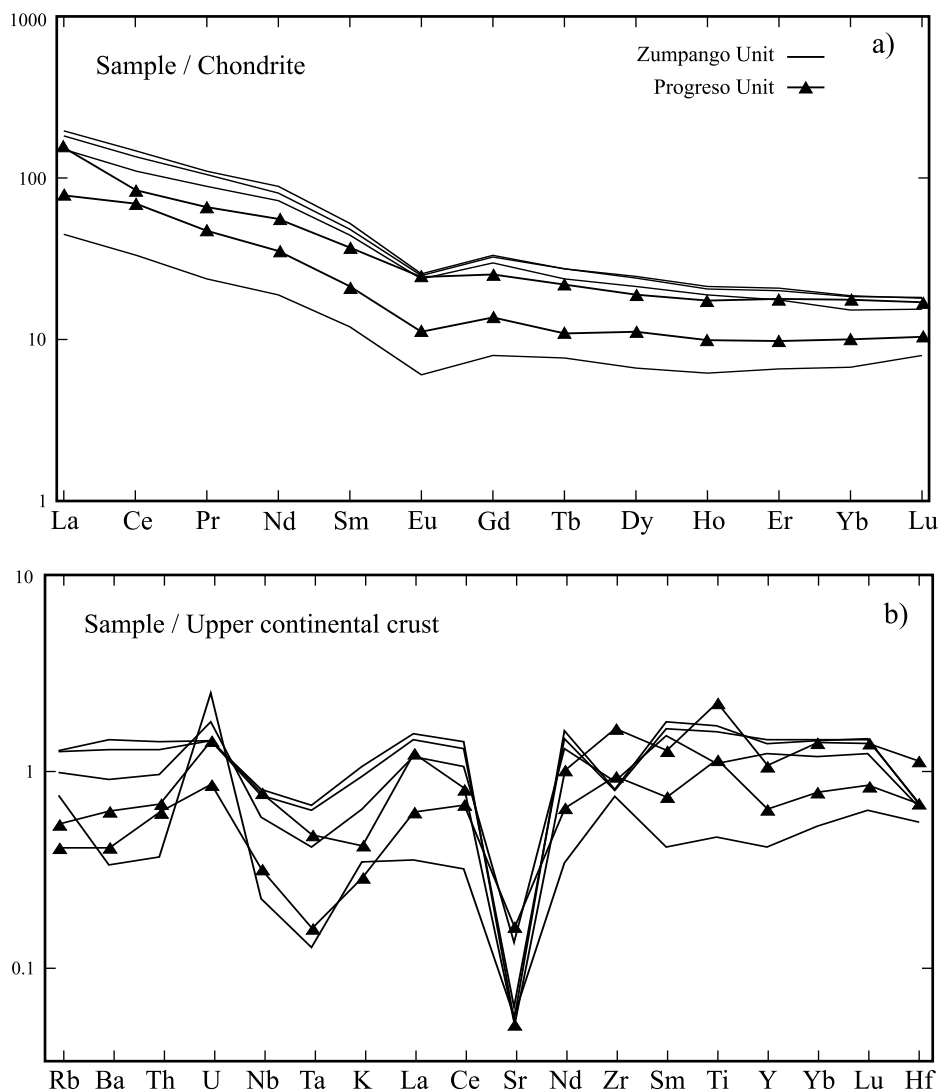


Figure 4. Chondrite- and upper continental crust- normalized plots of trace elements (Taylor and McLennan, 1985) from Zumpango and Progreso metasedimentary rocks.

(Table 1). In general, the variation observed in elements such as  $\text{TiO}_2$  and V is typical of a tholeiitic trend (Figure 6a and e). Ni content ranges from 90 to 156 ppm and Cr content ranges from 250 to 374 ppm. Ni and Cr display a slight negative correlation with Mg#.  $\text{Fe}_2\text{O}_3/\text{MgO}$  ranges from 1.2 to 3.6 with a high  $\text{Fe}_2\text{O}_3^{\dagger}$  (between 9.7 and 13.6 wt %) and a moderately high  $\text{TiO}_2$  content (between 1.0 and 1.7 wt %) contents. These features are also typical of tholeiitic mafic rocks as exemplified by the tholeiitic Skaergaard intrusion (Boudreau and McBirney, 1997; Figure 6f).

The mafic rocks are generally characterized by low Nb/Y (between 0.11 and 0.34), and are therefore subalkalic in composition (Figure 7a). These ratios are typical of either volcanic arc or mid-ocean ridge basalts (MORB). However, on a V vs. Ti/1000 discrimination diagram (Figure 7b), the samples clearly exhibit MORB-type characteristics.

On the Th-Hf-Ta diagram (Figure 8), the Olinalá

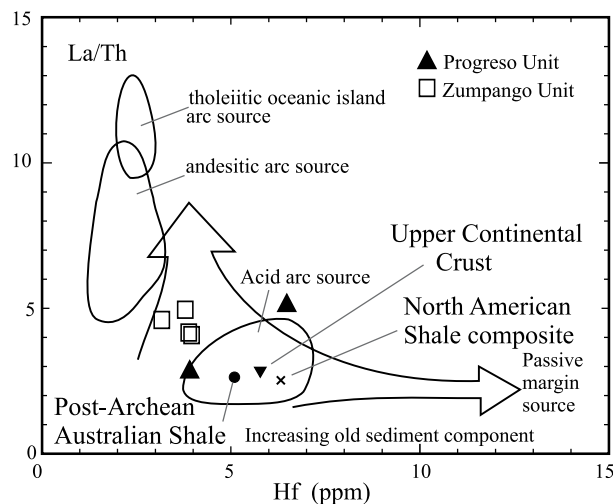


Figure 5. La/Th vs. Hf (ppm) diagram (after Floyd and Leveridge, 1987) for the metasedimentary rocks of the Zumpango and Progreso units.

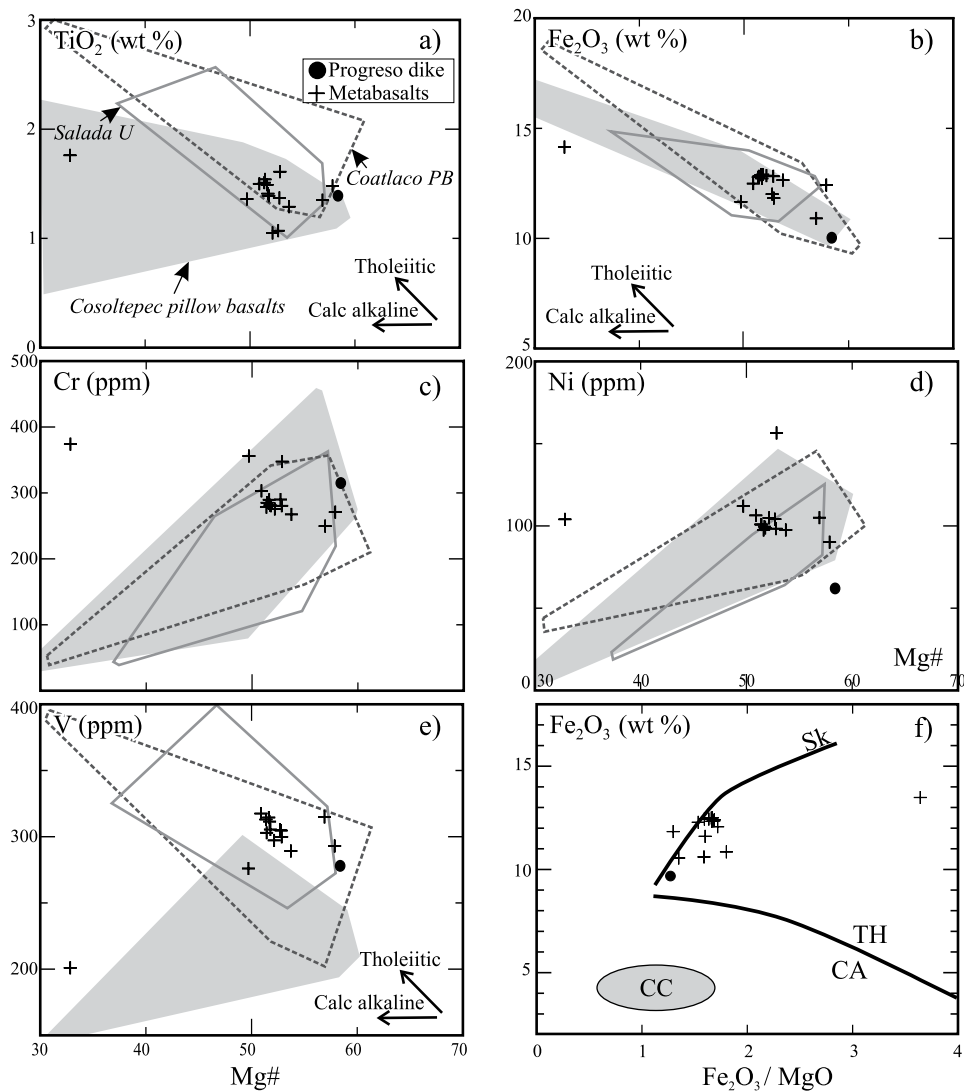


Figure 6. Major and trace element vs. Mg# plots and  $\text{Fe}_2\text{O}_3/\text{MgO}$  vs.  $\text{SiO}_2$  (trend lines after Miyashiro, 1974) of the Progreso Unit mafic rocks. Sk: Skaergaard trend, CC: continental crust (Tatsumi, 2005). Fields of published data for pillow basalts in the Coatlaco Unit (Grodzicki *et al.*, 2008) and Cosoltepec Fm. (Keppie *et al.* 2007), as well as for Carboniferous mafic dikes in the Salada Unit (Morales-Gómez *et al.*, 2009) are shown for comparison. See text for discussion.

samples plot in the N-MORB field. Relative abundances of the less mobile trace elements suggest a within plate to ocean floor tectonic setting.

On the Ta/Yb vs. Ce/Yb and diagram, most samples cluster very close to the mantle array (Figure 9) suggesting negligible contamination from either crustal or arc sources contamination. A few samples plot significantly above the mantle array indicating either a subduction component in the source or crustal contamination. Cr-Y abundances (Figure 10) suggest that the mantle source for the mafic rocks underwent 5–25% partial melting followed by minor fractionation of mafic phases.

Most, but not all, pillow basalts display no LREE enrichment (Figure 11a), with La/Sm<sub>N</sub> varying between 0.93 and 1.8. The low La/Yb<sub>N</sub> values (1.3 to 2.8) together with the low Nb/Y suggest derivation from a spinel lherzolite

mantle. The lack of a significant Eu anomaly indicates that plagioclase fractionation was relatively minor. Spider diagrams normalized to N-MORB indicate a slight enrichment of large ion lithophile elements (LILE) and absence of Nb or Ta negative anomalies (Figure 11b). This is consistent with other evidence indicating minimal contamination by either crustal or subduction components. The pillow basalts also display positive and negative anomalies in Sr, probably related to plagioclase alteration.

In general, the pillow basalts from Olinalá area have similar trends to those pillow basalts of the Coatlaco Unit south of Olinalá (Grodzicki *et al.*, 2008) and to the Carboniferous mafic dikes in the Salada Unit in the eastern Acatlán complex (Morales-Gómez *et al.*, 2009).

Sm-Nd analyses of the pillow basalts of the Naranjo block display a wide range of  $\epsilon\text{Nd}$  values (from +0.4 to +9.5;

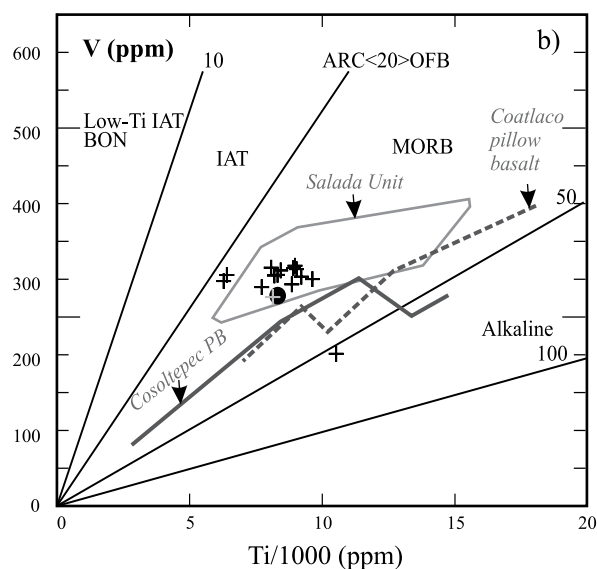
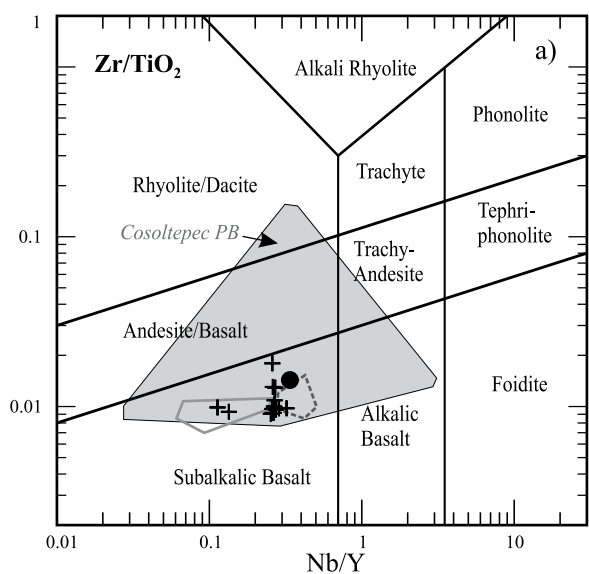


Figure 7. a: Nb/Y vs. Zr/Ti discrimination diagram (after Winchester and Floyd, 1977; Pearce, 1996) for Olinalá Carboniferous mafic and felsic rocks (Progreso and Zumpango units). b: Ti/1000 vs. V discriminant plot for mafic rocks of Olinalá area (Progreso and Zumpango units)(after Shervais, 1982). IAT: Island arc tholeiite; BON: boninite; MORB: mid-ocean ridge basalt. Symbols and fields as in Figure 6.

$t = 330$  Ma; Figure 12a, Table 2). Two samples (OL36-1 and OL36-2) have a higher  $\epsilon_{Nd}$  (+8.9 and +9.5, respectively) than the depleted mantle model (De Paolo, 1981) for the same age. Samples have high  $^{147}\text{Sm}/^{144}\text{Nd}$  ratios ranging from 0.1860 to 0.2442 (Figure 12b; Table 2) and thus their model age calculations are too imprecise to be relevant to this study (see Stern, 2002). Only sample OL500M1 (a highly deformed pillow basalt) has a relatively low ratio ( $^{147}\text{Sm}/^{144}\text{Nd} = 0.1545$ ) and a model age of 1.5 Ga (Table 2), suggesting that the source rocks was old sub-continental lithospheric mantle (e.g., Murphy and Dostal, 2007).

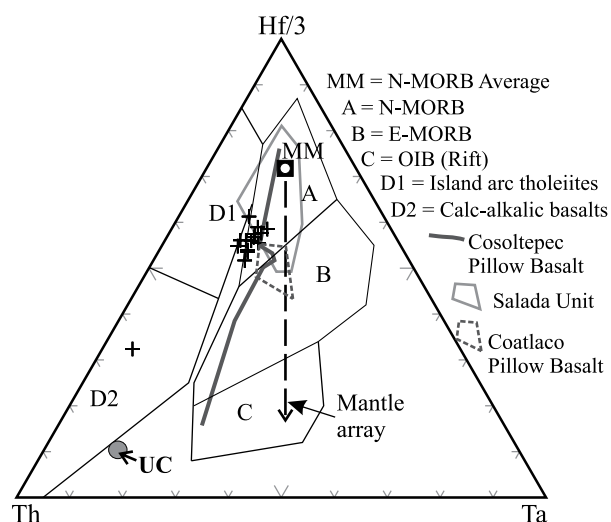


Figure 8. Tectonic setting discrimination in the Hf-Th-Ta diagram (after Wood *et al.*, 1979) for the Olinalá mafic rocks (Progreso and Zumpango units). UC: upper crust. Other symbols as in Figure 6.

## DISCUSSION AND CONCLUSIONS

The geochemistry of Carboniferous mafic rocks of the El Naranjo block, west of Olinalá indicates that they are tholeiitic with N-MORB characteristics and were derived from asthenospheric mantle (e.g., Figures 3 to 7). They lack evidence of significant fractionation or crustal contamination. These basalts show close petrological and geochemical similarities with coeval basalts from the Coatlace area (Grodzicki *et al.*, 2008) located ~3 km to the east of Olinalá, and also with sparse mafic dikes that

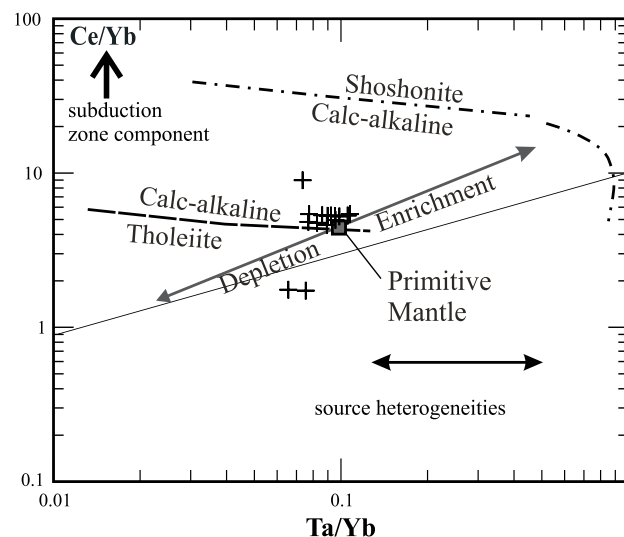


Figure 9. Plot of Ta/Yb vs. Ce/Yb used to identify subduction or crustal components and sources (after Pearce, 1982) in the Olinalá mafic rocks (Progreso and Zumpango units). Symbols as in Figure 6.

intrude the Carboniferous Salada Unit (Morales-Gómez *et al.*, 2009).

The high  $\epsilon\text{Nd}$  values are also characteristic for several Devonian and Carboniferous ophiolites in the Variscan orogen, including the Morais complex (Pin *et al.*, 2006), the Lizard complex (Davies *et al.*, 1984), Aracena (Castro *et al.*, 1996) and Massif Central (Pin and Paquette, 2002), which are all characterized by  $\epsilon\text{Nd}$  values that are equivalent to or slightly higher than the isotopic composition of the contemporary depleted mantle (DePaolo, 1981, 1988) suggesting derivation from a depleted mantle source (Murphy *et al.*, 2010).

The fact that these mafic rocks are interbedded with a thick sequence of continental-derived clastic rocks suggests likely that they formed on the margin of a continent rather than in an open oceanic environment (*cf.* Keppie *et al.*, 2006). This scenario is consistent with the occurrence of a crustally-derived Ordovician granitoid pluton in the Naranjo block (near Olinalá), which contains *ca.* 1 Ga zircons derived from a source similar to the Oaxacan complex that most probably underlies most of the Acatlán complex (*e.g.*, Keppie *et al.*, 2008a, 2008b; Ortega-Obregon *et al.*, 2009). Based on youngest detrital zircon age ( $403 \pm 7$  Ma; Ortega-

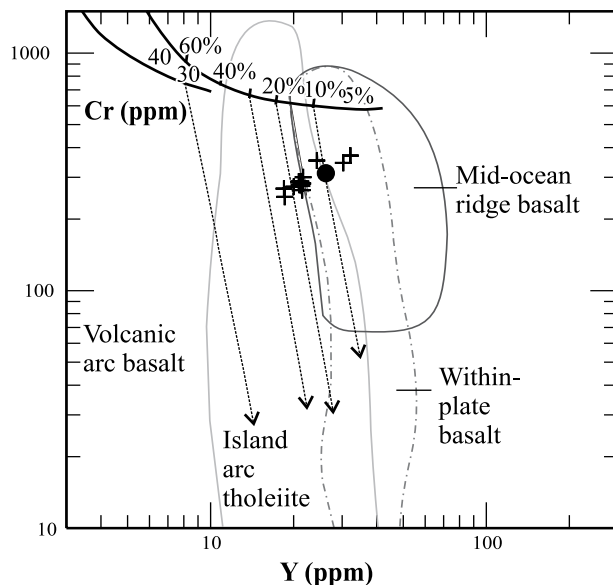


Figure 10. Cr-Y plot to identify the tectonic setting and the percent of melting (after Pearce, 1982) of the source from which the mafic magma of the Olinalá mafic rocks (Progreso and Zumpango units) were derived. Symbols as in Figure 6.

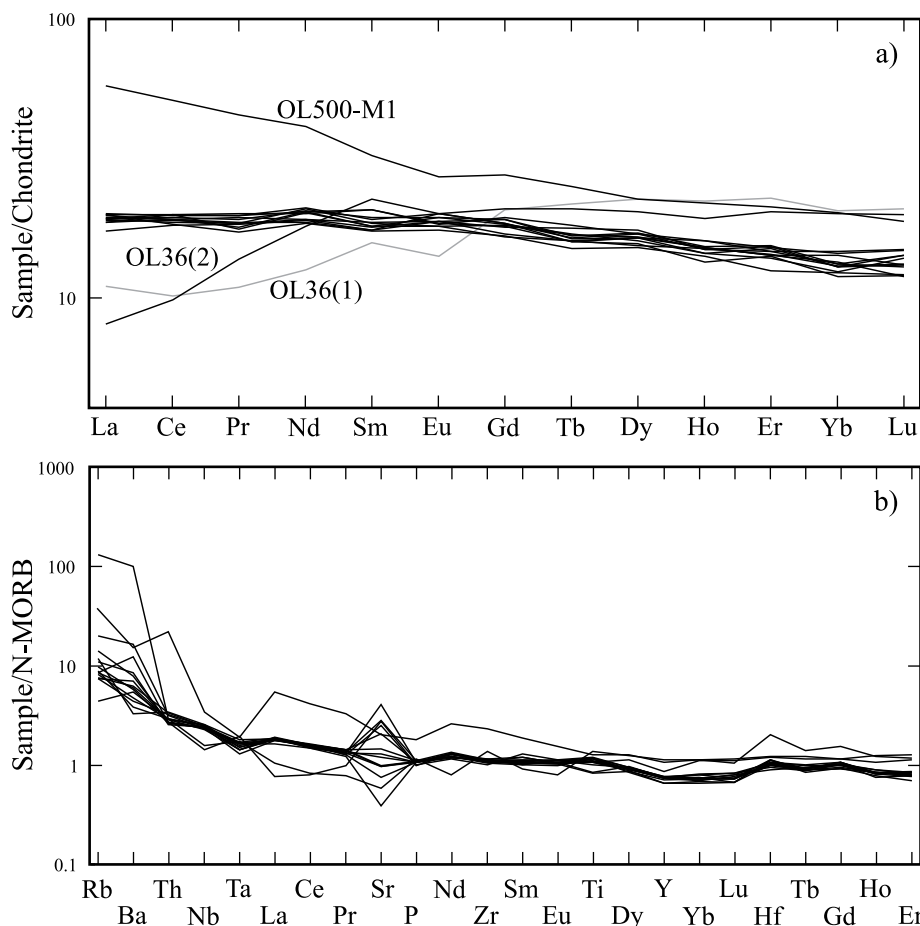


Figure 11. REE and trace element values of mafic rocks of the Progreso and Zumpango units normalized to (a) chondrite and (b) N-MORB. Normalizing values from Sun and McDonough, (1989).

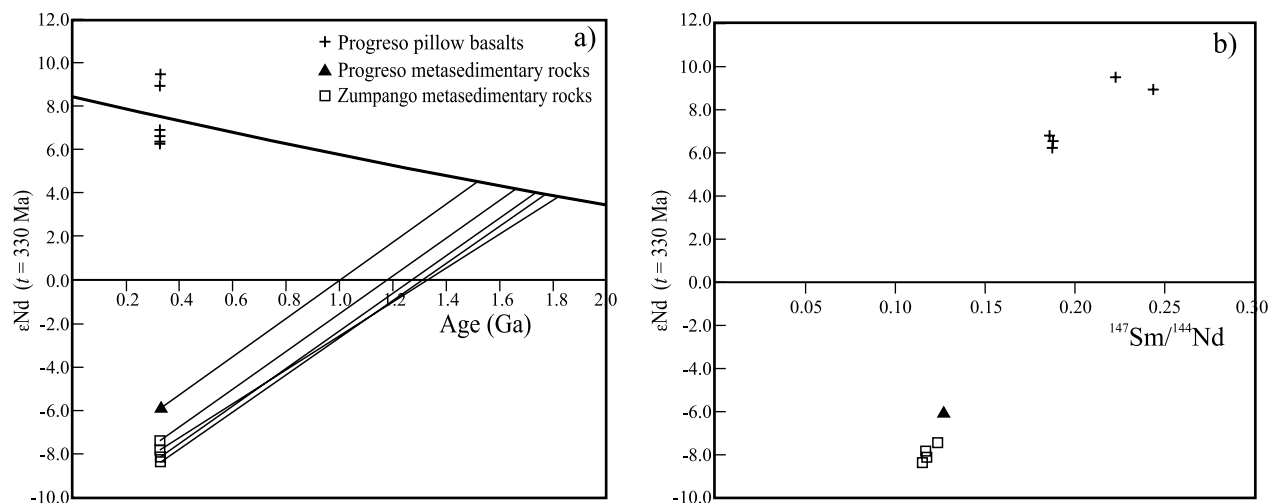


Figure 12. Sm-Nd isotopic data for representative magmatic rocks of the Olinalá area (Progreso and Zumpango units). a:  $\epsilon_{Nd}$  vs. model age plot, b:  $^{147}\text{Sm}/^{144}\text{Nd}$  vs.  $\epsilon_{Nd}$  data from metaigneous rocks are shown at  $t = 330$  Ma. Depleted-mantle model ages were calculated using a modern depleted-mantle composition of  $^{143}\text{Nd}/^{144}\text{Nd} = 0.513114$  and  $^{147}\text{Sm}/^{144}\text{Nd} = 0.213$  (see DePaolo, 1988).

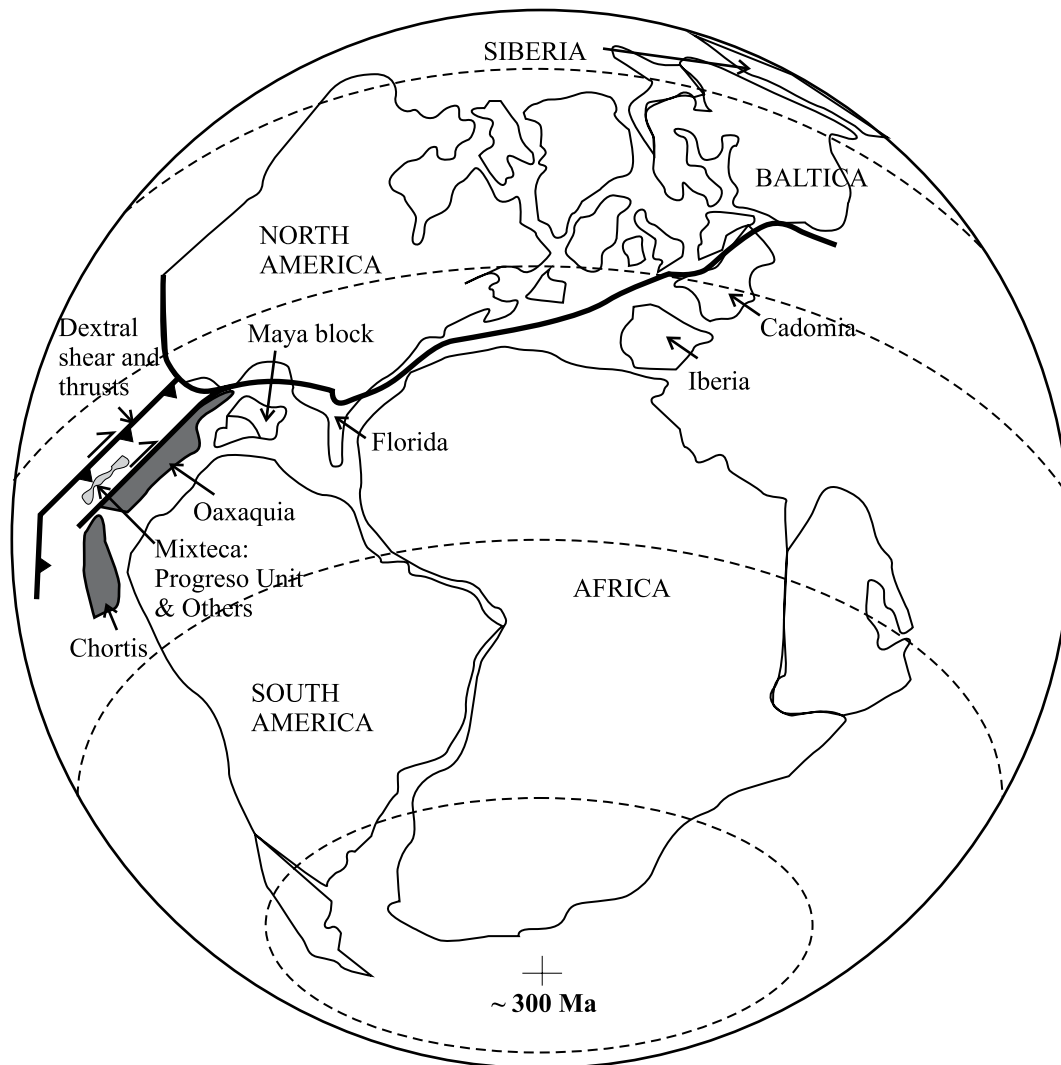


Figure 13. Paleogeographic reconstruction for the Permian-Carboniferous showing the probable position of sedimentation of Progreso Unit and extrusion of interbedded pillow basalts (modified from Keppie *et al.*, 2008a).

Obregón *et al.*, 2009), deposition of the Progreso Unit (in the Naranjo block) occurs within the Mississippian.

The age of one horizon in the Zumpango Unit is best constrained by the  $327 \pm 3$  Ma U-Pb age of the youngest concordant zircon in a felsic tuff interbedded with the clastic rocks. The angular unconformity of the overlying Olinalá Formation, suggests a pre-Middle Permian minimum depositional age. The age of the felsic source is indicated by the predominant detrital zircons ages: Oaxacan complex for the Progreso Unit, Neoproterozoic Maya block with a lesser contribution from the Oaxacan complex for the Naranjo and Zumpango units.

Deposition of the Progreso and Zumpango units is regarded by Keppie *et al.* (2008a, 2008b) as coeval with deformation associated with extrusion of high-pressure rocks into the Acatlán complex in an active tectonic margin (Ramos-Arias *et al.*, 2009). Extrusion of high pressure rocks is a process that occurs only in an active margin setting. Thus the rift setting suggested by the geochemistry probably indicates extension during extrusion. Furthermore, Keppie *et al.* (2008b) have proposed that the Devonian-Carboniferous arc was removed by subduction erosion: remnants occur as Devonian-Carboniferous igneous detrital zircons, and in high-pressure extruded rocks (*e.g.*, Meza-Figueroa *et al.*, 2005; Galaz *et al.*, 2009). Paleogeographic reconstructions consistent with paleomagnetic data (Figure 13; Keppie *et al.*, 2008a, 2008b and references therein; Morales-Gómez *et al.*, 2009) indicate that this active margin is probably the western margin of Pangea, as suggested by the Mid-continent (USA) affinities of Mississippian fauna found above the Oaxacan complex (Navarro-Santillán *et al.*, 2002), which presumably underlies the Acatlán complex (Keppie *et al.*, 2008b, Ortega-Obregón *et al.*, 2009, 2010).

## ACKNOWLEDGEMENTS

We thank CONACyT (Project CB-2005-1: 24894), PAPIIT (IN 100108-3) and NSERC for grants to support the work reported in this paper. COO was supported during his PhD by a CONACYT scholarship. JBM acknowledges the continuing support of NSERC (Canada) via Discovery and Research Capacity Development grants. We thank Drs. Peter Schaaf and Ricardo Vega-Granillo for their constructive comments.

## REFERENCES

Boudreau, A.E., McBirney, A.R., 1997, The Skaergaard Layered Series. Part III. Non-dynamic layering: *Journal of Petrology*, 38(8), 1003-1020.

Castro, A., Fernández, C., De la Rosa, J.D., Moreno Ventas, I., Rogers, G., 1996, Significance of MORB-derived amphibolites from the Aracena metamorphic belt, southwest Spain: *Journal of Petrology*, 37(2), 235-260.

Cullers, R. L., 1994, The controls on the major and trace element variation of shale, siltstone and sandstone of Pennsylvanian-Permian

age from uplifted continental blocks in Colorado to platform sediment in Kansas, USA: *Geochimica et Cosmochimica Acta*, 58(22), 4955-4972.

- Davies, G.R., 1984, Isotopic evolution of the Lizard Complex: *Journal of the Geological Society of London*, 141(1), 3-14.
- DePaolo, D., 1981, Trace element and isotopic effects of combined wallrock assimilation and fractional crystallization: *Earth and Planetary Science Letters*, 53(2), 189-202.
- DePaolo, D.J., 1988, Age dependence of the composition of continental: evidence from Nd isotopic variations in granitic rocks: *Earth and Planetary Science Letters*, 90, 263-271.
- Dostal, J., Keppie, J.D., 2009, Geochemistry of low-grade clastic rocks in the Acatlán Complex of southern Mexico: evidence for local provenance in felsic-intermediate igneous rocks: *Sedimentary Geology*, 222(3-4), 241-253.
- Dostal, J., Dupuy, C., Caby R., 1994, Geochemistry of the Neoproterozoic Tilemsi belt of Iforas (Mali, Sahara): a crustal section of an oceanic island arc: *Precambrian Research*, 65(1-4), 55-69.
- Floyd, P.A., Leveridge, B.E., 1987, Tectonic environment of the Devonian Gramscatho basin, south Cornwall: framework mode and geochemical evidence from turbiditic sandstone: *Journal of Geological Society*, 144(4), 531-542.
- Galaz, G., Keppie, J. D., Solari, L., 2009, Complejo Acatlán en el área de Tehuiztzingo, Estado de Puebla, sur de México: evidencias de su evolución tectónica (resumen) en Reunión Anual de la Unión Geofísica Mexicana, Puerto Vallarta, Jal.: 48-49.
- Girty, G.H., Ridge, D.L., Knaack, C., Johnson, D., Al-Riyami, R.K., 1996, Provenance and depositional setting of Paleozoic chert and argillite, Sierra Nevada, California: *Journal of Sedimentary Research*, 66(1), 107-118.
- Grodzicki, K.R., Nance, D., Keppie, J.D., Dostal, J., Murphy, J.B., 2008, Structural, geochemical and geochronological analysis of metasedimentary and metavolcanic rocks of the Coatlico area, Acatlán Complex, southern Mexico: *Tectonophysics*, 461(1-4), doi:10.1016/j.tecto.2008.01.016
- Jacobsen, S.B., Wasserburg, G.J., 1980, Sm-Nd isotopic evolution of chondrites: *Earth and Planetary Science Letters*, 50, 139-155.
- Jenner, G.A., Longerich, H.P., Jackson, S.E., Fryer, B.J., 1990, ICP-MS; a powerful tool for high-precision trace-element analysis in earth sciences; evidence from analysis of selected U.S.G.S. reference samples: *Chemical Geology*, 83(1-2), 133-148.
- Keppie, J.D., Ramos A.V., 1999, Odyssey of terranes in the Iapetus and Rheic oceans during the Paleozoic, in Ramos V.A., Keppie J.D. (Eds.), *Laurentia-Gondwana connections before Pangea*: Boulder, Colorado, Geological Society of America, Special Paper, 336, 267-275.
- Keppie, J.D., Nance, R.D., Fernandez-Suarez, J., Storey, C.D., Jefferies, T.E., Murphy, J.B., 2006, Detrital Zircon data from the eastern Mixteca terrane, southern Mexico: evidence for an Ordovician-Mississippian continental rise and a Permo-Triassic clastic wedge adjacent to Oaxaquia: *International Geology Review*, 48(2), 97-111.
- Keppie, J. D., Dostal, J., Elías-Herrera, M., 2007, Ordovician-Devonian oceanic basalts in the Cosoltepec Formation, Acatlán Complex, southern México: Vestiges of the Rheic Ocean?: *Geological Society of America, Special Paper* 423, 477-487.
- Keppie, J.D., Dostal, J., Miller, B.V., Ramos-Arias, M.A., Morales-Gomez, M., Nance, R.D., Murphy, J.B., Ortega-Rivera, A., Lee, J.W.K., Houston, T., Cooper, P., 2008a, Ordovician-earliest Silurian rift tholeiites in the Acatlán Complex, southern Mexico: Evidence of rifting on the southern margin of the Rheic Ocean: *Tectonophysics*, 461(1-4), doi:10.1016/j.tecto.2008.01.010
- Keppie, J.D., Dostal, J., Murphy, B., Nance, D., 2008b, Synthesis and tectonic interpretation of the westernmost Paleozoic Variscan orogen in southern Mexico: From rifted Rheic margin to active Pacific margin: *Tectonophysics*, 461(1-4), doi:10.1016/j.tecto.2008.01.012
- Kerr, A., Jenner, G.A., Fryer, B.J., 1995, Sm-Nd isotopic geochemistry of Precambrian to Paleozoic granitoid suites and the deep-crustal structure of the southeast margin of the Newfoundland Appalachians: *Canadian Journal of Earth Sciences*, 32,

- 224-245.
- Longerich, H.P., Jenner, G.A., Fryer, B.J., Jackson, S.E., 1990, Inductively coupled plasma-mass spectrometric analysis of geological samples: A critical evaluation based on case studies: *Chemical Geology*, 83, 105-118.
- Matte, P., 2001, The Variscan collage and orogeny (480–290 Ma) and the tectonic definition of the Armorica microplate: a review: *Terra Nova*, 13(2), 122-128.
- Meza-Figueroa, D., Ruiz, J., Talavera-Mendoza, O., Ortega-Gutiérrez, F., 2005, Tectono-metamorphic evolution of the Acatlán Complex eclogites (southern Mexico). *Canadian Journal of Earth Sciences* 40, 27–44.
- Miyashiro, A., 1974, Volcanic rock series in island arcs and active continental margins: *American Journal of Science*, 274, 321-355.
- Morales-Gómez, M., Keppie, J.D., Dostal, J., 2009, Carboniferous tholeiitic dikes in the Salada Unit, Acatlán Complex, southern Mexico: a record of extension on the western margin of Pangea: *Revista Mexicana de Ciencias Geológicas*, 26(1), 136-142.
- Murphy, J.B., Dostal, J., 2007, Continental mafic magmatism of different ages in the same terrane: constraints on the evolution of an enriched mantle source: *Geology*, 35(4), 335-338.
- Murphy, J.B., Keppie, J.D., Dostal, J., Waldron, J.W.F., Cude, M.P., 1996, Geochemical and isotopic constraints on the accretion of the Avalonia in the Appalachian-Caledonide orogen: evidence from Early Silurian clastic sequences in Antigonish Highlands, Nova Scotia, Canada: *Canadian Journal of Earth Sciences*, 33, 379-388.
- Murphy, J.B., Keppie, J.D., Braid, J.A., Nance, R.D., 2005, Geochemistry of the Tremadocian Tiñu Formation (Southern Mexico): provenance in the underlying ~1 Ga Oaxacan complex on the southern margin of the Rheic Ocean: *International Geology Review*, 47(9), 887-900.
- Murphy, J.B., Keppie, J.D., Nance, R.D., Dostal, J., 2010, Comparative evolution of the Iapetus and Rheic oceans: a North American perspective: *Gondwana Research*, 17(2-3), 482-499.
- Nance, R.D., Miller, B.V., Keppie, J.D., Murphy, J.B., Dostal, J., 2006, Acatlán Complex, southern Mexico: record spanning the assembly and breakup of Pangea: *Geology*, 34, 857-860.
- Nance, R.D., Miller, B.V., Keppie, J.D., Murphy, J.B., Dostal, J., 2007, Vestige of the Rheic Ocean in North America: the Acatlán Complex of southern Mexico, *In* Linnemann, U., Nance, R.D., Zulauf, G., Kraft, P. (Eds.), *The Geology of Peri-Gondwana: The Avalonia-Cadomian Belt, Adjoining Cratonic and the Rheic Ocean*: Boulder, Colorado, Geological Society of America, Special Paper, 423, 437-452.
- Navarro-Santillán, D., Sour-Tovar, F., Centeno-García, E., 2002, Lower Mississippian (Osagean) brachiopods from the Santiago Formation, Oaxaca, Mexico: stratigraphic and tectonic implications: *Journal of South American Earth Sciences*, 15(3), 327-336.
- Ortega-Gutiérrez, F., Elías-Herrera, M., Reyes-Salas, M., Macías-Romo, C., López, R., 1999, Late Ordovician–Early Silurian continental collision orogeny in southern Mexico and its bearing on Gondwana–Laurentia connections: *Geology*, 27(8), 719-722.
- Ortega-Obregón, C., Keppie, J.D., Murphy, J.B., Lee, J.K.W., Ortega-Rivera, A., 2009, Geology and geochronology of Paleozoic rocks in western Acatlán Complex, southern Mexico: evidence for contiguity across an extruded high-pressure belt and constraints on Paleozoic reconstructions: *Geological Society of America Bulletin*, 121(11-12), 1678-1694.
- Ortega-Obregón, C., Keppie, J.D., Murphy, J.B., 2010, Geochemistry and Sm–Nd isotopic systematics of Ediacaran–Ordovician, sedimentary and bimodal igneous rocks in the western Acatlán Complex, southern Mexico: Evidence for rifting on the southern margin of the Rheic Ocean: *Lithos*, 114(1-2), 155-167.
- Pearce, J.A., 1982, Trace element characteristics of lavas from destructive plate margins, *in* Thorpe, R.S. (ed.), *Andesites: Orogenic andesites and related rocks*: London, John Wiley & Sons, 525-548.
- Pearce, J.A., 1996, A user's guide to basalt discrimination diagrams, *in* Wyman, D.A. (ed.), *Trace element geochemistry of volcanic rocks: Applications for massive sulphide exploration*. Geological Association of Canada, Short Course Notes 12, 79-114.
- Pin, C., Paquette, J.L., 2002, Le magmatisme basique calcoalcalin d'âge dévono-dinantien du nord du Massif Central, témoin d'une marge active hercynienne: arguments géochimiques et isotopiques Sr/Nd: *Geodinamica Acta*, 15(1), 63-77.
- Pin, C., Paquette, J.L., Ábalos, B., Santos-Zalduegui, J.F., Gil-Ibarguchi, J.I., 2006, Composite origin of an early Variscan transported suture: Ophiolitic units of the Morais Nappe Complex (north Portugal): *Tectonics*, 25, doi:10.1029/2006TC001971
- Ramírez-Espinoza, J., 2001, Tectono-magmatic evolution of the Paleozoic Acatlán complex in southern Mexico and its correlation with the Appalachian system: Arizona, Arizona University, Ph. D. Thesis, 171 pp.
- Ramos-Arias, M., Keppie, J. D., Valencia, V., 2009, Análisis estructural y geocronología U-Pb en Ixcamilpa de Guerrero, Puebla, oeste del Complejo Acatlán sur de México: implicaciones en la exhumación de rocas de alta presión (abstract): *GEOS* 29(1), p. 49.
- Shervais, J.W., 1982, Ti–V plots and the petrogenesis of modern and ophiolitic lavas: *Earth and Planetary Science Letters*, 59(1), 101-118.
- Stern, R.J., 2002, Crustal evolution in the East African Orogen: a neodymium isotopic perspective: *Journal of African Earth Sciences*, 34 (3-4), 109-117.
- Sun, S.S., McDonough, W.F., 1989, Chemical and isotopic systematics of oceanic basalts: implications for mantle composition and processes, *in* Saunders, A.D. Norry, M.J. (Eds.), *Magmatism in the Ocean Basins*: London, Geological Society, Special Publications, 42, 313-345.
- Talavera-Mendoza, O., Ruiz, J., Gehrels, G.E., Meza-Figueroa, D.M., Vega-Granillo, R., Campa-Uranga, M.F., 2005, U-Pb geochronology of the Acatlán Complex and implications for the Paleozoic paleogeography and tectonic evolution of southern Mexico: *Earth and Planetary Science Letters*, 235(3-4), 682–699. doi: 10.1016/j.epsl.2005.04.013.
- Tatsumi, Y., 2005, The subduction factory; how it operates in the evolving Earth: *Geology Society of America Today*, 15(7), 4-10.
- Taylor, S.R., McLennan, S.M., 1985, *The continental crust: its composition and evolution*: United States, Blackwell Scientific Publications, Oxford, 312 pp.
- Vachard, D., Flores de Dios, A., 2002, Discovery of latest Devonian / earliest Mississippian microfossils in San Salvador Patlanoaya (Puebla, Mexico): Biogeographic and geodynamic consequences: *Comptes Rendus Geoscience*, 334, 1095–1101.
- Vachard, D., Flores de Dios, A., Pantoja, J., Buitrón, B.E., Arellano, J., Grajales, M., 2000, Les fusulines du Mexique, une revue biostratigraphique et paléogéographique: *Geobios*, 33(6), 655-679.
- Vega-Granillo, R., Talavera, M.O., Meza-Figueroa, D., Ruiz, J., Gehrels, G., López, M., De la Cruz, V.J.C., 2007, Pressure-temperature-time evolution of Paleozoic high-pressure rocks of the Acatlán Complex (southern Mexico): Implications for the evolution of the Iapetus and Rheic Oceans: *Geological Society of America Bulletin*, 119(9-10), 1249-1264.
- Winchester, J.A., Floyd, P.A., 1977, Geochemical discrimination of different magma series and their differentiation products using immobile elements: *Chemical Geology*, 20, 325–343. doi: 10.1016/0009-2541(77)90057-2.
- Winchester, J.A., Pharaoh, T.C., Verniers, J., 2002, Palaeozoic amalgamation of Central Europe: an introduction and synthesis of new results from recent geological and geophysical investigations, *in* Verniers, J. (Ed.), *Palaeozoic amalgamation of Central Europe*: London, Geological Society of London Special Publication, 201, 1-18.
- Wood, D.A., Joron, J.L., Treuil, M., Norry, M., Tarney, J., 1979, Elemental and Sr isotope variations in basic lavas from Iceland and the surrounding ocean floor: *Contributions to Mineralogy and Petrology*, 70(3), 319-339.

Manuscript received: November 6, 2009

Corrected manuscript received: March 11, 2010

Manuscript accepted: March 23, 2010